Minimum-Weight Analysis of Filamentary Composite Wide Columns

LESLIE M. LACKMAN*
North American Rockwell Corporation, Los Angeles, Calif.

AND

ROBERT M. AULT†
Stresskin Products Company, a Division of Tool Research and Engineering Corporation, Santa Ana, Calif.

A minimum-weight analysis of an integrally stiffened filamentary composite wide column is presented. The analysis satisfies both strength and torsional stiffness requirements. The buckling coefficient for the longitudinal stiffener (i.e., an orthotropic plate with three sides simply supported and one side free) is determined. The analysis accounts for the filament cross-ply angle of the sheet and the longitudinal stiffening of the stiffener. The efficiency of the integrally stiffened filamentary composite wide column is shown to be competitive with a Y-stiffened wide column constructed from the matrix material.

Nomenclature

A = enclosed area = $b \times h$
b = spar spacing
b_s = stiffener spacing
D_1, D_2 = flexural rigidities in x and y directions, respectively
D_3 = twisting rigidity
E_x, E_y = Young's modulus in x and y directions, respectively
F_{cy} = compression yield
G_{xy} = shear modulus
h = spar depth
h_s = stiffener depth
J = torsional constant
K_s = stiffener buckling coefficient
L = rib spacing
M_x, M_y, M_{xy} = internal moment components
N_x, N_y, N_{xy} = internal load components
$\bar{N}_x$ = applied load intensity
t = sheet thickness
t_s = stiffener thickness
$\bar{t}$ = weight effective thickness
u, v, w = displacement components
V_f = filament volume fraction
γ = $4G_{xy}{}^s(1 - \nu_{xy}{}^s\nu_{xy}{}^s)/E_y{}^s + \nu_{xy}{}^s$
$\epsilon_x, \epsilon_y, \epsilon_{xy}$ = strain components
θ = filament cross-ply angle
ν_{xy} = Poisson's ratio, relating strain in the y direction to strain in x direction due to stress in x direction
ν_{yx} = Poisson's ratio, relating strain in the x direction to strain in y direction due to stress in y direction
ρ = material density
ρ_f = density of face sheet
ρ_s = density of stiffener
$\sigma_x, \sigma_y, \sigma_{xy}$ = stress components

Subscripts

x, y, z = coordinates
0 = midplane of sheet
cr = critical

Superscripts

f = face
s = stiffener

Received January 27, 1967; revision received November 1, 1967.

* Member of the Technical Staff, Advanced Structures Group. Member AIAA.

† Senior Engineer; formerly with North American Rockwell Corporation. Member AIAA.

Introduction

RECENTLY, Dow, Rosen, and Kingsbury,[1] and Rosen and Dow[2] have reported the results of studies performed to evaluate the potential of aerospace structures composed of composite materials. These studies indicate that aerospace structural components, e.g., shear webs, compression covers, fuselage shells, and beams, fabricated with filamentary composite materials offer significant weight reductions when compared to the same components fabricated from advanced structural metals.

The analysis presented herein treats the minimum-weight analysis of an integrally stiffened filamentary composite wide column. The buckling coefficient for the longitudinal stiffener (i.e., for an orthotropic plate with three sides simply supported and one side free) is determined. The analysis accounts for a variable filament cross-ply angle of the basic sheet and its effect on the minimum-weight configuration is shown.

The wide-column stiffened skin construction shown in Fig. 1a is the model considered. This construction was chosen because it possesses the desired characteristics of an efficient compression structure, i.e., relative to its weight it has high flexural rigidity parallel to the loading and support directions, and is relatively simple to analyze. The wide-column structure is further assumed to be the top cover of a wing box structure. In addition to strength, the box structure is required to satisfy aerodynamic torsional stiffness requirements. The torsional stiffness values used in this study were based on estimated stiffness requirements for future aerospace lifting vehicles.

The stiffeners are assumed to be reinforced by uniaxial continuous filaments, while the face sheet is considered to be a laminated composite reinforced by filaments orientated in a symmetric pattern in the plane of the laminates. Fig. 1b illustrates the filament reinforcing for a typical skin and stiffener element of the wide-column construction.

Theoretical Development

Stress-Strain Relations

The elastic stress-strain relations for an orthotropic sheet in a state of plane stress are:

$$\epsilon_x^f = \sigma_x^f/E_x^f - \nu_{yx}^f\sigma_y^f/E_y^f$$
$$\epsilon_y^f = \sigma_y^f/E_y^f - \nu_{xy}^f\sigma_x^f/E_x^f \qquad \epsilon_{xy}^f = \sigma_{xy}^f/2G_{xy}^f \tag{1}$$

Only four of the elastic constants of Eq. (1) are independent; by employing Maxwell's reciprocal theorem, the relation between the dependent and independent constants can be shown to be

$$\nu_{xy} = (E_x/E_y)\nu_{yx} \tag{2}$$

With the assumption that the plate stiffeners resist only the deformation of the plate in their stiffening direction, the stiffeners' stress-strain relation is expressed by

$$\epsilon_x^s = \sigma_x^s/E_x^s \tag{3}$$

Strain-Displacement Relations

Assuming that sections plane before bending remain plane after bending; the components of displacements at a distance z from the midsurface of the sheet are

$$u(z) = u_0 - \left(\frac{\partial w}{\partial x}\right)z \qquad v(z) = v_0 - \left(\frac{\partial w}{\partial y}\right)z$$
$$w(z) = w \tag{4}$$

Assuming the gradients of the normal displacements to be small, the strain-displacement relationships are expressed as

$$\epsilon_x = \partial u(z)/\partial x = \partial u_0/\partial x - (\partial^2 w/\partial x^2)z$$
$$\epsilon_y = \partial v(z)/\partial y = \partial v_0/\partial y - (\partial^2 w/\partial y^2)z$$
$$\epsilon_{xy} = [\partial v(z)/\partial x + \partial u(z)/\partial y]/2 = 1/2[\partial u_0/\partial y + \partial v_0/\partial x - 2(\partial^2 w/\partial x\partial y)z] \tag{5}$$

Internal Forces and Moments

The internal forces and moments per unit width (Fig. 2) are defined as

$$N_x = \left[\int_{-(h_s+t/2)}^{t/2}\int_{-b_s/2}^{b_s/2}\sigma_x dydz\right]\Big/ b_s$$
$$M_x = \left[\int_{-(h_s+t/2)}^{t/s}\int_{-b_s/2}^{b_s/2}\sigma_x z dydz\right]\Big/ b_s$$
$$N_y = \int_{-t/2}^{t/2}\sigma_y dz \qquad M_y = \int_{-t/2}^{t/2}\sigma_y z dz$$
$$N_{xy} = \int_{-t/2}^{t/2}\sigma_{xy} dz \qquad M_{xy} = \int_{-t/2}^{t/2}\sigma_{xy} z dz \tag{6}$$

Substitution of Eqs. (1, 3, and 5) into Eq. (6) and performing the indicated integration yields

$$N_x = \frac{E_x^s t_s[h_s\partial u_0/\partial x + (th_s + h_s^2)(\partial^2 w/\partial x^2)/2]}{b_s} + \frac{E_x^f t[\partial u_0/\partial x + \nu_{yx}^f\partial v_0/\partial y]}{(1 - \nu_{xy}^f\nu_{yx}^f)} \tag{7a}$$

$$N_y = \frac{E_y^f t[\partial v_0/\partial y + \nu_{xy}^f\partial u_0/\partial x]}{(1 - \nu_{xy}^f\nu_{yx}^f)} \tag{7b}$$

$$N_{xy} = G_{xy}^f t[\partial v_0/\partial x + \partial u_0/\partial y] \tag{7c}$$

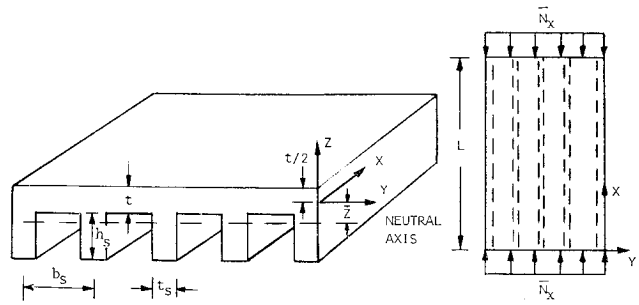

Fig. 1a Wide-column construction and loading diagrams.

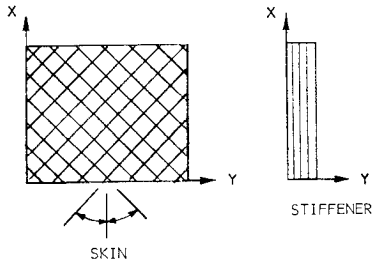

Fig. 1b Typical filamentary reinforcement.

$$M_x = -(E_x^s t_s/b_s)[(h_s + t)h_s(\partial u_0/\partial x)/2 + h_s(h_s^2/3 + h_s t/2 + t^2/4)(\partial^2 w/\partial x^2)] - \frac{E_x^f t^3[\partial^2 w/\partial x^2 + \nu_{yx}^f\partial^2 w/\partial y^2]}{12(1 - \nu_{xy}^f\nu_{yx}^f)} \tag{7d}$$

$$M_y = \frac{-E_y^f t^3[\partial^2 w/\partial y^2 + \nu_{xy}^f\partial^2 w/\partial x^2]}{12(1 - \nu_{xy}^f\nu_{yx}^f)} \tag{7e}$$

$$M_{xy} = -G_{xy}^f t^3(\partial^2 w/\partial x\partial y)/6 \tag{7f}$$

Equations of Equilibrium

If we consider a compressive force $\bar{N}_x$ applied to the plate shown in Fig. 1a, and neglect the changes in the in-plane forces due to the plate's buckling displacements, the equilibrium equation for the plate in its buckled position is[3]

$$\partial^2 M_x/\partial x^2 + 2\partial^2 M_{xy}/\partial x\partial y + \partial^2 M_y/\partial y^2 = \bar{N}_x\partial^2 w/\partial x^2 \tag{8a}$$

The additional strains $\partial u_0/\partial x$, and $\partial v_0/\partial y$ produced by the buckling of the plate can be solved for in terms of the plate's curvatures by invoking the aforementioned condition that no in-plane forces are introduced during buckling. Thus, setting Eqs. (7a–7c) equal to zero, solving for the strain $\partial u_0/\partial x$ in terms of $\partial^2 w/\partial x^2$, substituting this result into Eqs. (7d–7f), and then substituting Eqs. (7d–7f) into Eq. (8a) yields

$$D_1\partial^4 w/\partial x^4 + 2D_3\partial^4 w/\partial x^2\partial y^2 + D_2\partial^4 w/\partial y^4 = -\bar{N}_x\partial^2 w/\partial x^2 \tag{8b}$$

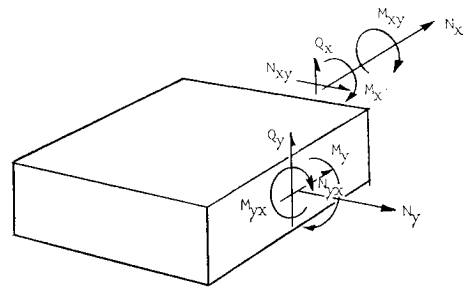

Fig. 2 Positive directions of internal forces and moments.

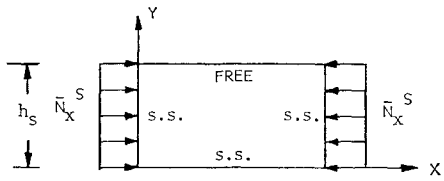

Fig. 3 Stiffener loading and boundary conditions.

where

$$D_1 = \frac{E_x^s h_s t_s\{-(h_s + t)^2/4[1 + E_x^f b_s t/E_x^s t_s h_s] + h_s^2/3 + h_s t/2 + t^2/4\}}{b_s} + \frac{E_x^f t^3}{12(1 - \nu_{xy}^f \nu_{yx}^f)}$$

$$D_2 = E_y^f t^3/12(1 - \nu_{xy}^f \nu_{yx}^f)$$

$$D_3 = G_{xy}^f t^3/6 + t^3(E_y^f \nu_{xy}^f + E_x^f \nu_{yx}^f)/24(1 - \nu_{xy}^f \nu_{yx}^f)$$

General Instability

With the substitution of the appropriate buckled mode shape into Eq. (8b), the critical buckling load for an integral stiffened composite plate can readily be obtained. However, in this discourse we will concern ourselves only with wide-column construction; hence, Eq. (8b) becomes

$$D_1 d^4w/dx^4 + \bar{N}_x d^2w/dx^2 = 0 \tag{9}$$

Assuming $w = A \sin m\pi x/L$, where L is the column's length, substitution of this relation into Eq. (9) and solving for the minimum buckling load yields

$$(\bar{N}_x)_{cr} = \pi^2 D_1/L^2 \tag{10}$$

Local Instability

In addition to the general instability mode of failure, the stiffened skin construction can fail by local buckling of its sheet and stiffener elements. Replacing $\bar{N}_x$ in Eq. (8b) by $\bar{N}_x^f$, i.e., the component of the compression load which is resisted by the face sheet, setting b_s and h_s equal to zero, and substituting the resulting flexural and torsional stiffness relations into Eq. (8b) yields

$$D_1^f \partial^4w/\partial x^4 + 2D_3^f \partial^4w/\partial x^2\partial y^2 + D_2^f \partial^4w/\partial y4 = -\bar{N}_x^f \partial^2w/\partial x^2 \tag{11}$$

where

$$D_1^f = E_x^f t^3/12(1 - \nu_{xy}^f \nu_{yx}^f)$$

$$D_2^f = E_y^f t^3/12(1 - \nu_{xy}^f \nu_{yx}^f)$$

$$D_3^f = G_{xy}^f t^3/6 + t^3(\nu_{yx}^f E_x^f + \nu_{xy}^f E_y^f)/24(1 - \nu_{xy}^f \nu_{yx}^f)$$

Treating the face sheet as a series of infinitely long, simply supported, orthotropic plates, the face sheet's buckling allowable as obtained from Eq. (11) is found from Ref. 3 to be

$$(\bar{N}_x^f)_{cr} = 2\pi^2[(D_1^f D_2^f)^{1/2} + D_3^f]/b_s^2 \tag{12}$$

Buckling of the plate stiffeners is another possible local instability mode of failure. Considering this element to be a plate with three sides simply supported and one side free, as shown in Fig. 3, the appropriate stability equation is obtained by replacing t with t_s and the superscripts f by s in Eq. (11). Assuming the plate buckles into one sinusoidal half-wave in the longitudinal direction, the solution to the modified Eq. (11) is sought in the form,

$$w = f(y) \sin\pi x/a \tag{13}$$

where $a = L$. Substituting Eq. (13) into the modified Eq. (11), the following ordinary differential equation for $f(y)$ is obtained:

$$\frac{d^4f}{dy^4} - 2\left(\frac{D_3^s}{D_2^s}\right)\left(\frac{\pi}{a}\right)^2 \frac{d^2f}{dy^2} + \left[\left(\frac{D_1^s}{D_2^s}\right)\left(\frac{\pi}{a}\right)^4 - \left(\frac{\bar{N}_x^s}{D_2^s}\right)\left(\frac{\pi}{a}\right)^2\right] f = 0 \tag{14}$$

Noting that because of the constraints along the sides $y = o$ and $y = h_s$

$$(\bar{N}_x^s)_{cr} > D_1^s(\pi/a)^2$$

the solution to Eq. (14) becomes

$$f(y) = C_1 \sinh\alpha y + C_2 \cosh\alpha y + C_3 \sin\beta y + C_4 \cos\beta y \tag{15a}$$

where C_1–C_4 are constants of integration, and

$$\beta = \bar{\beta}/h_s \qquad \alpha = \bar{\alpha}/h_s$$

$$\bar{\beta} = [(\pi h_s)/a]^{1/2}\{[(D_3^s/D_2^s)^2(\pi h_s/a)^2 - (D_1^s/D_2^s)(\pi h_s/a)^2 + (\bar{N}_x^s h_s^2/D_1^s)(D_1^s/D_2^s)]^{1/2} - (D_3^s/D_2^s)(\pi h_s/a)\}^{1/2}$$

$$\bar{\alpha} = [(\pi h_s)/a]^{1/2}\{[(D_3^s/D_2^s)^2(\pi h_s/a)^2 - (D_1^s/D_2^s)(\pi h_s/a)^2 + (\bar{N}_x^s h_s^2/D_1^s)(D_1^s/D_2^s)]^{1/2} + (D_3^s/D_2^s)(\pi h_s/a)\}^{1/2}$$

Since the side of the plate along $y = o$ is simply supported, and the side along $y = h_s$ is free, the boundary conditions for the stiffener element are

at $y = o$,

$$w = o \qquad \partial^2w/\partial y^2 + \nu_{xy}^s \partial^2w/\partial x^2 = 0 \tag{15b}$$

at $y = h_s$

$$\partial^2w/\partial y^2 + \nu_{xy}^s \partial^2w/\partial x^2 = 0 \tag{15c}$$

$$\partial^3w/\partial y^3 + (\partial^3w/\partial x^2\partial y)[4G_{xy}^s(1 - \nu_{xy}^s\nu_{yx}^s)/E_y^s + \nu_{xy}^s] = 0$$

Substitution of Eq. (13) into Eqs. (15b) and (15c) and setting the determinant of the resulting equations equal to zero yields the following transcendental equation:

$$\bar{\beta}[\bar{\beta}^2 + (\pi h_s/a)^2\gamma][\bar{\alpha}^2 - (\pi h_s/a)^2\nu_{xy}^s] \tanh\bar{\alpha} = \bar{\alpha}[\bar{\alpha}^2 - (\pi h_s/a)^2\gamma][\bar{\beta}^2 + (\pi h_s/a)^2\nu_{xy}^s] \tan\bar{\beta} \tag{16}$$

Considering the stiffeners to be infinitely long, i.e., $h_s/a \to o$, the critical load for this local mode of failure can be expressed as

$$(\bar{N}_x^s)_{cr} = K_s D_1^s/h_s^2 = K_s E_x^s t_s^3/[12(1 - \nu_{xy}^s\nu_{yx}^s)h_s^2] \tag{17}$$

where K_S is a nondimensional buckling coefficient whose value is determined from Eq. (16).

Axial Load Distribution

The axial compression load $\bar{N}_x$ is assumed to be applied at the plate's neutral axis; thus producing a prebuckled uniform contraction of the stiffened skin construction. Because of differences in the axial stiffness of the sheet and stiffener, the

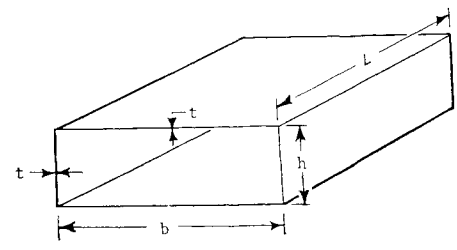

Fig. 4 Simple torque box.

stress or in-plane load of these elements are different. Equations (18a) relate the load carried by the sheet and stiffener to the axial compression load $\bar{N}_x$ which is applied at the plate's neutral axis;

$$\bar{N}_x{}^f = \frac{\bar{N}_x t E_x{}^f}{[E_x{}^s h_s t_s/b_s + E_x{}^f t]} \qquad \bar{N}_x{}^s = \frac{\bar{N}_x t_s E_x{}^s}{[E_x{}^s h_s t_s/b_s + E_x{}^f t]} \tag{18a}$$

The distance from the coordinate axis to the column's neutral axis is denoted by $\bar{z}$ (see Fig. 1a), and

$$\bar{z} = E_x{}^s t_s(h_s{}^2 + h_s t)/\{2b_s[E_x{}^s h_s t_s/b_s + E_x{}^f t]\} \tag{18b}$$

Torsional Stiffness

The torsional stiffness expression for the simple torque box shown in Fig. 4 is[4]

$$GJ = 2A^2 G_{xy}{}^f t/(b + h) \tag{19}$$

where (GJ) is the box's torsional stiffness; the webs are assumed to have the same thickness and shear modulus as the cover sheets; the torsional stiffness of the cover stiffeners were neglected; and A is the cross-sectional area of the bay, i.e., $A = bh$.

Hence, for a given $(GJ)_{\text{req}}$ the product of the face shear modulus with the ratio of the skin thickness to the cover's rib spacing must satisfy

$$G_{xy}{}^f(t/L) = K = (GJ)_{\text{req}}/[2A^2 L/(h + b)] \tag{20}$$

Based on a study of the requirements of future aircraft, a typical range for K is 16,000–100,000 psi.

Optimization Procedures

Simultaneous Buckling Modes

The weight effective thickness of the wide-column construction can be expressed as

$$(\bar{t}/L) = [1 + (\rho_s/\rho_f)(h_s/t)(t/b_s)(t_s/t)](t/L) \tag{21}$$

In keeping with established minimum-weight analysis theory, the requirement for a minimum-weight structure is simultaneous local and general buckling. Hence, to insure simultaneous local buckling of both the face sheet and stiffener elements, we require that

$$(\bar{N}_x{}^f)_{\text{cr}}/(\bar{N}_x{}^s)_{\text{cr}} = \bar{N}_x{}^f/\bar{N}_x{}^s \tag{22}$$

Substitution of Eqs. (12, 17, and 18) into Eq. (22) yields

$$(t_s/t) = \psi_1(h_s/t)(t/b_s) \tag{23}$$

where

$$\psi_1 = [2(E_x{}^s/E_x{}^f)(\phi_f/\phi_s)]^{1/2}\pi$$

$$\phi_f = (E_x{}^f E_y{}^f)^{1/2}/12(1 - \nu_{xy}{}^f\nu_{yx}{}^f) + G_{xy}{}^f/6 + (\nu_{yx}{}^f E_x{}^f + \nu_{xy}{}^f E_y{}^f)/24(1 - \nu_{xy}{}^f\nu_{yx}{}^f)$$

$$\phi_s = K_s E_x{}^s/12(1 - \nu_{xy}{}^s\nu_{yx}{}^s)$$

Equating the stiffener local buckling allowable, Eq. (17), to the applied compression load for the stiffener element, Eq. (18a), results in

$$(t_s/h_s) = \{\bar{N}_x E_x{}^s/[\phi_s(E_x{}^s h_s t_s/b_s + E_x{}^f t)]\}^{1/2} \tag{24}$$

Substituting Eq. (23) into Eq. (24) and rearranging yields

$$(h_s/t) = \{(\bar{N}_x/L)E_x{}^s(b_s/t)^2/[\phi_s(t/L)\psi_1{}^2] - E_x{}^f\}^{1/2}(b_s/t)/(E_x{}^s\psi_1)^{1/2} \tag{25}$$

To insure simultaneous local and general buckling, the applied load per inch must equal the allowable load per inch as defined by Eq. (10). Rearranging Eq. (10) into parametric form, we have

$$\frac{N_x}{L} = \pi^2\left(\frac{t}{L}\right)^3\left\{E_x{}^s\left(\frac{t_s}{t}\right)\left(\frac{t}{b_s}\right)\times\left[\frac{\frac{h_s}{t}\left[1+\frac{h_s}{t}\right]^2}{4\left[1+\left(\frac{E_x{}^f}{E_x{}^s}\right)\left(\frac{b_s}{t}\right)\left(\frac{t}{t_s}\right)\left(\frac{t}{h_s}\right)\right]}+\frac{\left(\frac{h_s}{t}\right)^3}{3}+\frac{\left(\frac{h_s}{t}\right)^2}{2}+\frac{\left(\frac{h_s}{t}\right)}{4}\right]+\frac{E_x{}^f}{12(1-\nu_{xy}{}^f\nu_{yx}{}^f)}\right\} \tag{26}$$

Minimum-Weight Analysis

The objective of the minimum-weight analysis is to minimize the parametric effective thickness, Eq. (21), for a given load index $\bar{N}_x/L$. For a given stiffener-sheet combination, this equation involves four independent parameters, namely, 1) (h_s/t), 2) (t/b_s), 3) (t_s/t), and 4) (t/L).

However, the auxiliary relations that insure simultaneous occurrence of general instability, local face instability, and local stiffener instability reduce the minimization procedure to making variations with respect to one independent parameter, such as (t/L).

If the geometric parameters are constrained according to Eq. (23), simultaneous buckling of the stiffener and sheet, between stiffeners, is guaranteed. This can be seen by a simple manipulation of Eq. (23) which shows that ψ_1 is the ratio of the sheet to stiffener width to thickness ratios. Mathematically,

$$\psi_1 = (b_s/t)/(h_s/t_s)$$

To insure that the applied stress equals the local allowable stress, the geometric parameters must be constrained in accordance with Eq. (25).

Simultaneous general and local buckling is guaranteed by the solution of Eq. (26), which must be solved by iteration. The minimization was performed with respect to (t/L). Therefore, for a given $(\bar{N}_x/L)$ and (t/L), the solution of Eq. (26) is accomplished by iterating on (b_s/t) with (h_s/t) computed from Eq. (25) and (t_s/t) from Eq. (23). Once, the value of b_s/t is found which satisfies Eq. (26), a new value for (t/L) is taken and the iteration process is repeated.

Following each solution of Eq. (26), (t/L) is computed from Eq. (21). Hence, for a given $(\bar{N}_x/L)$, the minimization is performed by determining the value of $(\bar{t}/L)$ which yields the minimum value of $(\bar{t}/L)$. This procedure must be repeated for each cross-ply angle.

Material Properties

The elastic material properties for the sheet and stiffener can be determined from the relations presented in Refs. 5 and 6. These relations are a function of the elastic materials constants of the matrix and filaments, filament volume fraction, filament orientation, and correspond to the composite elastic material relations based on constituent properties proposed by Hill,[7] Tsai,[8] Paul,[9] Hashin and Rosen,[10] Whitney and Riley,[11] Greszczuk,[12] and others. The elastic constants given in Table 1 are for an extensional type of deformation; however, they will also be used to represent the flexural elastic constants for the cross-plied face sheet of the stiffened skin construction. This is a reasonable approximation for this study, since the face sheet, in general, will contain many plies and the error introduced by using the aforementioned constants in calculating the flexural stiffness terms will be small. Table 1 shows the material properties used in this analysis.

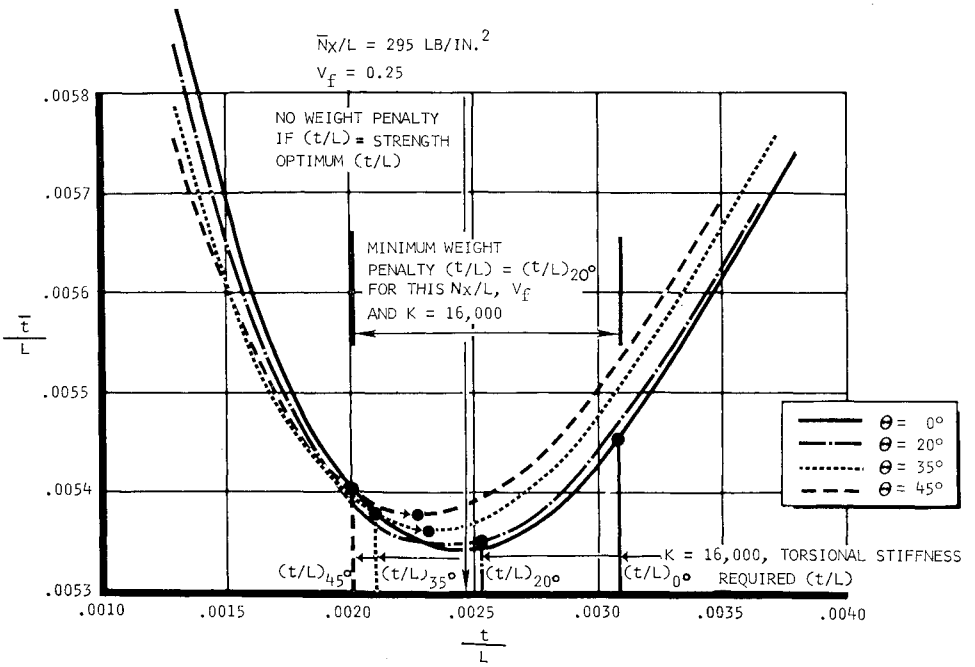

Fig. 5 Torsional stiffness constraint weight penalty determination.

Torsional Stiffness Constraint

The previously described minimization process yields the lightest structure for a given load index. However, quite often torsional stiffness requirements demand face gages that exceed the skin thickness determined from the aforementioned analysis. The following procedure describes the modified approach for these cases.

For each cross-ply angle, the (t/L) required to satisfy the torsional stiffness requirements can be computed from Eq. (20) as $(t/L)_\theta = K/G_{xy}{}^f{}_\theta$. Consider a plot of $(\bar{t}/L)$ vs $(t/L)$for a given load index $(\bar{N}_x/L)$ with a family of constant cross-ply angles as shown in Fig. 5. Each point on these curves satisfies the strength requirements. For a given K, a list of (t/L) required can be computed for each cross-ply angle. Since the composite sheet shear modulus will be greatest for a cross-ply angle of $\pm 45°$,$(t/L)_{45°}$ required will be smaller than $(t/L)_\theta$ with $\theta < 45°$.

As can be seen from Fig. 5, when $(t/L)_\theta$ is less than or equal to the strength optimum (t/L), no weight penalty is required to satisfy torsional stiffness requirements. When (t/L) is greater than the strength optimum (t/L), the minimum-weight penalty is determined from the minimum point on the curve defined by the coordinates [(t/L) required for torsional stiffness; $(\bar{t}/L)$ required by strength requirements for appropriate θ]. These coordinate points are illustrated in Fig. 5 for $\bar{N}_x/L = 295$ lb/in.^{2}, $V_f = 0.25$ and $K = 16{,}000$. The minimum-weight penalty occurs for $\theta = 20°$.

Discussion of Results

Comparison of Minimum-Weight Concepts

A computer program was written employing the optimization procedure described in the previous section. Typical filamentary composite materials consisting of an X7002 aluminum matrix with boron filaments with a volume fraction of 0.25 and 0.35 were considered.

Figure 6 shows a plot of $(\bar{t}/L)$ vs $(\bar{N}_x/L)$ for the integrally stiffened filamentary composite wide column for filament volume fractions of 0, 0.25, and 0.35. Further, an efficiency plot is included for a Y-stiffened wide column constructed from the matrix material. This curve is based on data presented in Ref. 13, where this type of construction was found to have an efficiency factor of 1.23; on an efficiency basis, this was the second highest of the 16 wide-column configurations studied.

It can be seen from Fig. 6 that the filamentary composite integrally stiffened wide column with $V_f = 0.35$ is as efficient as the more sophisticated Y-stiffened construction. The analysis presented herein is purely elastic. However, to indicate the load index range of applicability of this analysis, the line corresponding to $F_{cy} = 63{,}000$ psi for the matrix

Table 1 Material properties (all moduli are $\times 10^{-6}$)

Element	Cross-ply θ	$E_x{}^a$	$E_x{}^b$	$E_y{}^a$	$E_y{}^b$	$G_{xy}{}^a$	$G_{xy}{}^b$	$\nu_{xy}{}^a$	$\nu_{xy}{}^b$	$\nu_{yx}{}^a$	$\nu_{yx}{}^b$	$K_s{}^a$	$K_s{}^b$
		Composite material properties											
Stiffener	0	22.72	27.70	15.42	17.04	5.19	5.79	0.255	0.237	0.173	0.146	2.55	2.32
Face sheet	0	22.72	27.70	15.42	17.04	5.19	5.79	0.255	0.237	0.173	0.146	...	...
Face sheet	±10	21.99	26.70	15.20	16.79	5.51	6.22	0.276	0.263	0.191	0.165	...	...
Face sheet	±20	20.02	24.00	14.63	16.15	6.32	7.32	0.330	0.328	0.242	0.221	...	...
Face sheet	±35	16.23	18.75	13.98	15.46	7.60	9.07	0.402	0.414	0.346	0.342	...	...
Face sheet	±45	14.50	16.30	14.50	16.28	7.92	9.50	0.397	0.406	0.397	0.406	...	...

Material	E	G	ν	ρ	K_s — Isotropic
	Constituent properties				
Matrix—X7002 aluminum	10.3	3.9	0.30	0.104	4.20 (for $V_f = 0$)
Filament—boron	60.0	26.8	0.12	0.090	4.20 (for $V_f = 0$)

[a] $V_f = 0.25$, 112 filaments/in., filament diam 0.004, 0.00567 ply thickness.
[b] $V_f = 0.35$, 120 filaments/in., filament diam 0.004, 0.0043 ply thickness.

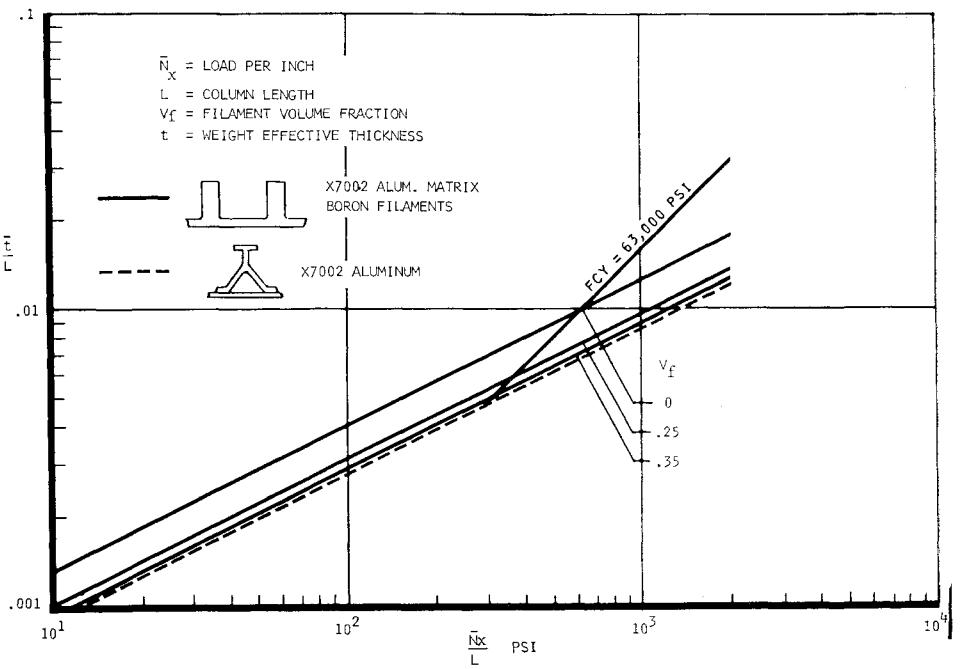

Fig. 6 Wide-column structural efficiency.

material is also plotted in Fig. 6. The matrix material F_{cy} was selected since a reliable analytical method for accurately determining the composite F_{cy} has not yet been established.

Effect of Torsional Stiffness Constraint

The weight penalty incurred when torsional stiffness requirements are satisfied is shown by Fig. 7 for selected values of K. This figure corresponds to $V_f = 0.25$. A similar figure can be constructed for each V_f.

In order to determine the geometry required for both the strength optimum and torsional stiffness constraint case, curves similar to Fig. 8 can be constructed for selected $\bar{N}_x/L$ values. The minimum-weight geometry required to meet strength requirements is determined from the (t/L) that produces the smallest value of $(\bar{t}/L)$. The corresponding values of (t_s/t), (h_s/t), and (b_s/t) can be read from the appropriate curves in Fig. 8.

To satisfy the torsional stiffness requirements, the (t/L) required for a given K is determined, and, using curves similar to those shown by Fig. 5, the minimum-weight penalty is determined by the procedure discussed earlier. The corresponding values of (t_s/t), (h_s/t), and (b_s/t) can be determined using curves similar to Fig. 8. Moreover, curves similar to Fig. 8 can be used to assess the weight penalty involved when minimum gage requirements preclude the use of the minimum weight (t/L).

It should be mentioned that in order to discuss the theoretically exact procedure for the minimum-weight analysis including torsional stiffness constraint, Fig. 5 has been constructed with a highly enlarged $(\bar{t}/L)$ scale. From a practical point of view, the differences in $(\bar{t}/L)$ for the various cross-ply angles are relatively insignificant.

Conclusions

1) An analytical procedure has been presented for determining the minimum-weight design of a filamentary composite integrally stiffened wide column satisfying both

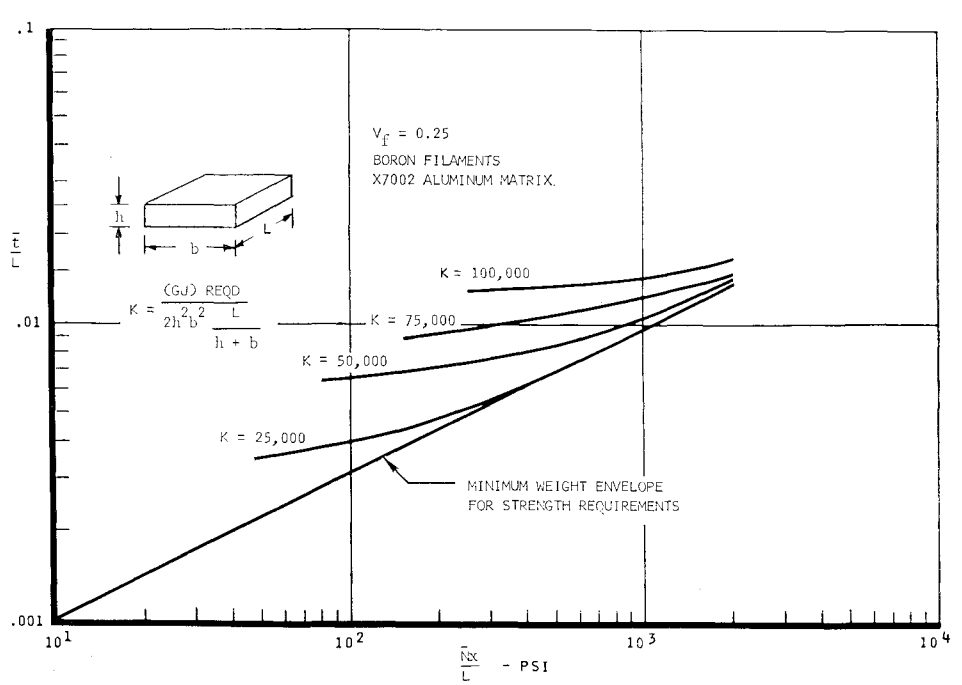

Fig. 7 Weight penalty required by torsional stiffness requirements.

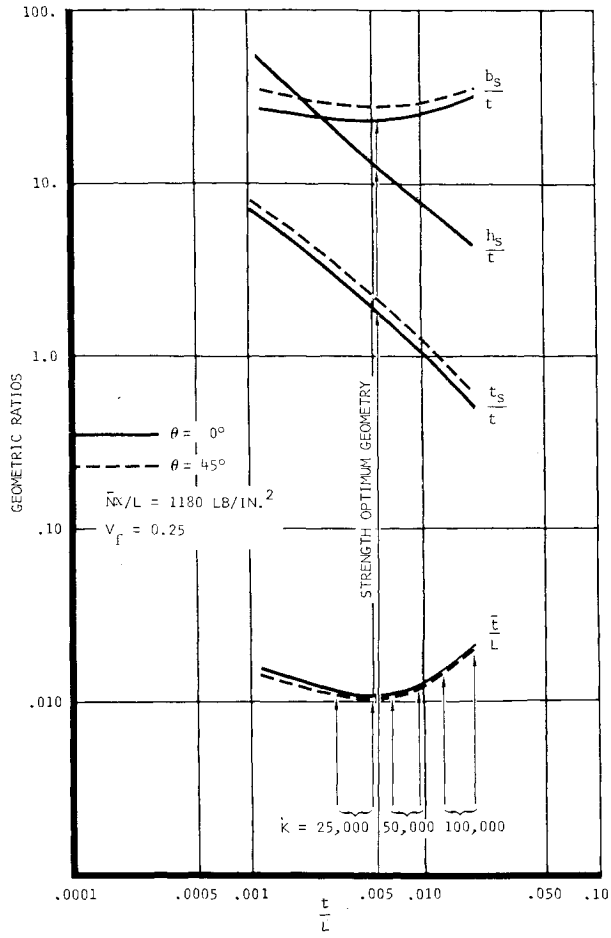

Fig. 8 Chart for determining nonoptimum geometry.

strength and torsional stiffness requirements. The filament cross-ply angle for the sheet material is accounted for in the analysis. The stiffeners are assumed to be reinforced by longitudinal filaments.

2) The transcendental equation for determining the buckling coefficient of an orthotropic plate with three sides simply supported and one side free has been determined. This equation has been solved for a long boron-X7002 aluminum filamentary composite plate with longitudinal filaments and filament volume fractions of 0.25 and 0.35. Buckling coefficients were found to be 2.55 and 2.32 for $V_f = 0.25$ and 0.35, respectively; as compared to 4.20 for an isotropic plate.

3) For small values of K, the sheet filament cross-ply angle has been shown to have a relatively insignificant effect on the weight parameter $(\bar{t}/L)$.

4) It has been shown that an integrally stiffened boron-aluminum filamentary composite wide column with a filament volume fraction of 0.35 is as efficient as a Y-stiffened aluminum type of construction.

5) A simple filamentary composite stiffened skin concept is competitive from a weight standpoint when compared to more sophisticated stiffening arrangements fabricated from the composite matrix material. The results of this analysis indicate that additional studies to evaluate the efficiency of compression elements fabricated from filamentary composite materials are warranted.

References

[1] Dow, N. F., Rosen, W., and Kingsbury, H. B., "Evaluation of the Potential of Advanced Composite Materials," MAC, March 31, 1966, Air Force Materials Lab.

[2] Rosen, B. W. and Dow, N. F., "Influence of Constituent Properties Upon the Structural Efficiency of Fibrous Composite Shells," *Journal of Spacecraft and Rockets*, Vol. 3, No. 9, Sept. 1966, pp. 1377–1384.

[3] Timoshenko, S. and Gere, J. M., *Theory of Elastic Stability*, McGraw-Hill, New York, 1961, Chap. 9.

[4] Perry, D. J., *Aircraft Structures*, McGraw-Hill, New York, 1950.

[5] Dickerson, E. O. and DiMartino, B., "Off-Axis Strength and Testing of Filamentary Materials for Aircraft Application," *Advanced Fibrous Reinforced Composites*, Vol. 10, H23–H50, Society of Aerospace Materials and Process Engineers, San Diego, Calif., Nov. 9–11, 1966.

[6] Lackman, L. M. and Ault, R. M., "Mechanical Properties of Filamentary Materials," Rept. NA65-431, 1965, North American Aviation Inc., Los Angeles Div., Los Angeles, Calif.

[7] Hill, R., "Elastic Properties of Reinforced Solids: Some Theoretical Principles," *Journal of Mechanics and Physics of Solids*, Vol. 11, 1963, pp. 357–372.

[8] Tsai, S. W., "Structural Behavior of Composite Materials," CR-71, July 1964, NASA.

[9] Paul, B., "Prediction of Elastic Constants of Multiphase Materials," *Transactions of the American Institute of Mining, Metallurgical, and Petroleum Engineers*, Vol. 219, 1960, pp. 36–41.

[10] Hashin, Z. and Rosen, B. W., "The Elastic Moduli of Fiber-Reinforced Materials," *Journal of Applied Mechanics*, June 1964, pp. 223–232.

[11] Whitney, J. M. and Riley, M. B., "Elastic Properties of Fiber-Reinforced Composite Materials," *AIAA Journal*, Vol. 4, No. 9, Sept. 1966, pp. 1537–1542.

[12] Greszcuk, L. B., "Elastic Constants and Analysis Method for Filament Wound Structures," Rept. RM-45849, Jan. 1964, Douglas Aircraft Co.

[13] Emero, D. H. and Spunt, L., "Optimization of Multirib and Multiweb Wing Box Structures under Shear and Moment Loads," *AIAA Sixth Structures and Materials Conference*, American Institute of Aeronautics and Astronautics, April 1965.